MNK Publication

International Journal of Latest Research in Science and Technology **ISSN (Online):2278-5299**
Volume 3, Issue 4: Page No.47-53. July-August 2014
https://www.mnkpublication.com/journal/ijlrst/index.php

CONTROL PARAMETERS OF ACTIVE MAGNETIC BEARINGS SUPPORTING ROTATING SYSTEMS

[1]Luiz de Paula do Nascimento, [2]Carlos Henrique de Oliveira Arantes,
[1]São Paulo State University - UNESP, Ilha Solteira, Brazil
[2]São Paulo State University - UNESP, Ilha Solteira, Brazil

Abstract- The intensity of the exciting force of rotating systems supported by active magnetic bearings is limited by the maximum load capacity of the bearings. Also, the maximum electrical current of control is limited by the saturation current of the ferromagnetic material of the bearing. The force and electrical current of control depend on the transfer function of the control circuit, which can vary as a function of the fitted parameters for the controller, normally a PID controller. At the design stage it is very important to carry out an analysis of these parameters. Therefore in this work a theoretical procedure to determine the force and control current of active magnetic bearing is presented. The theoretical results will be compared with experimental data to verify the accuracy of the procedure.

Keywords - Magnetic Bearing; Active Control; Control Parameter; Rotating System

I. INTRODUCTION

Active Magnetic Bearing (AMB) is a rather new concept in bearing technology. The AMBs are electromagnetic devices configured to suspend a shaft within a gap. The basic operating principles of AMBs are given in Allaire *et al.* [1]. They take radial loads or thrust loads by utilizing a magnetic field to support the shaft rather than a mechanical force as in fluid film or rolling element bearings. Overviews on active magnetic bearing applications have been presented by Kasarda [2] and Schweitzer and Maslen [3]. There is a considerable amount of literature on active control systems used for rotor vibration reduction employing magnetic actuator, for instance, Kuseyri [4], Shi *et al.* [5], Piper *et al.* [6] and Jang *et al.* [7]. Also, there are several interesting publications in which the authors use active control systems with magnetic actuator together with systems of fault control or fault diagnosis in turbo-machinery or rotor system. A theoretical analysis was performed by Zhu *et al.* [8] on dynamic characteristics of a cracked rotor with an active magnetic bearing. Cole *et al.* [9] consider a control system design for a rotor-magnetic bearing system that integrates a number of fault-tolerant control methods. In the design of magnetic bearings there are features such as size, stiffness and damping, control force, electrical current of control, dynamics and others that are under design limits. Because of the wide range of new applications of magnetic bearings nowadays, this subject has became of great interest and has already been addressed, for example, by Schweitzer [10] and Zingerli and Kolar [11]. Nevertheless, additional work should be conducted in this direction, including experimental analyzes. In this work a procedure to simulate the control force and control current of magnetic bearing based on its geometric characteristics and control parameters is presented. The precision of that procedure was verified by comparing theoretical and experimental results from an experimental rotor magnetic-bearings apparatus.

II. FEEDBACK CONTROL

An active control system is required to maintain stability of the magnetic bearing-rotor system. The controller takes signals provided by the sensors located adjacent to the actuators and computes the necessary stabilizing current request. Amplifiers then provide the requested current to the actuators, which creates the stabilizing electromagnetic forces. Low pass filter is also used in the plant controller to eliminate undesirable disturbances. This feedback loop is updated thousands of times per second. The Fig. (1) presents a block diagram of a single radial bearing control axis. In addition to the stabilizing feedback loop, open loop control can also be used to minimize unbalance-induced shaft whirl or minimize the vibration transmitted to the bearing houses. In open loop control, the active nature of the magnetic bearings is used to adaptively cancel the synchronous components of either the measured shaft position or the bearing current. It is important to note that open loop control alone cannot provide stable levitation; i.e., it only can be used once the system is stabilized through the feedback control action.

Figure 2 shows the basic geometry of an active magnetic bearing in a differential assembly. The air gap has thickness g and each horseshoe shaped section has area A_g. The magnetic forces in each magnet are generated by an electric current i flowing through N coils wound in the horseshoes. The Fig. 3 shows the action of these forces in a single control axis.

Publication History
Manuscript Received : ***31 August 2014***
Manuscript Accepted : ***31 August 2014***
Revision Received : ***31 August 2014***
Manuscript Published : ***31 August 2014***

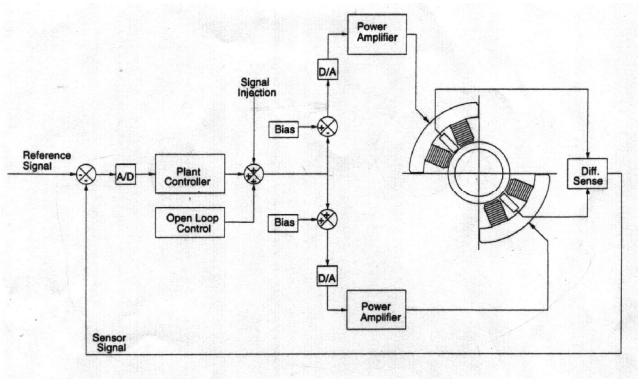

Fig. 1 Single axis closed loop control for radial bearing (Courtesy of Revolve Magnetic Bearing Inc.)

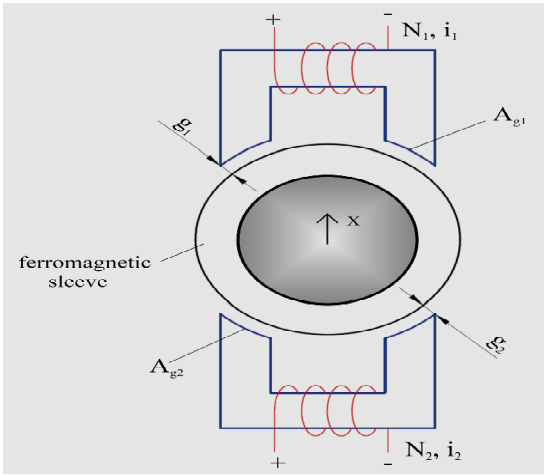

Fig. 2 Basic geometry of magnetic bearing in double action

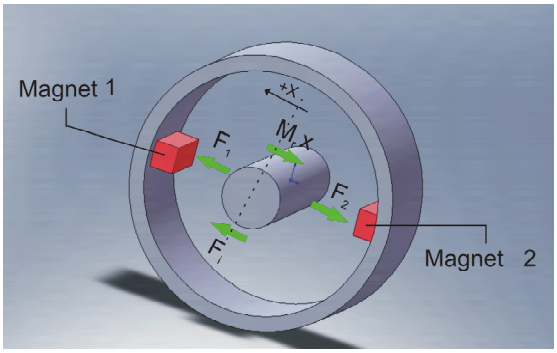

Fig. 3 Forces produced on the magnetic bearing

A. ***Magnetic force of control***

Forces of control of the active magnetic bearings basically depend on the design characteristics, displacement of the rotor and electrical current. As mentioned the forces are generated in each pole of the magnetic bearing by a rolling up of *N* coils with an electrical current passing through it. From the principles of magnetism, the force acting in each pole of the bearing can be determined according to the equation:

$$F = \varepsilon \frac{\mu_0 N^2 i^2 A_g}{4g^2} \quad (1)$$

where $\mu_0 = 4\pi x10^{-7} (Hm^{-1})$ is the permeability of the free space (air), g is the gap between the rotor and the stator, A_g is the area face of each pole and ε *is* the geometric correction factor evaluated as 0.8 for radial bearing due to electrical current flight effect. Once the electromagnetic forces are only of attraction, in each control axle, magnets must be positioned in both sides and diametrically opposite from the rotor, in a double action scheme, as shown in Figs. 2 and 3, in a manner that the net control force F_N in the bearing plane is given by:

$$F_N = F_2 - F_1 = \varepsilon \frac{\mu_0 N^2 A_g}{4} \left(\frac{i_2^2}{g_2^2} - \frac{i_1^2}{g_1^2} \right) \quad (2)$$

The stability of the rotor in its centered position during the control process is achieved by making the electrical current in each magnet as follows:

$$i_1 = i_s - i_c \quad ; \quad i_2 = i_s + i_c \quad (3)$$

where i_s is a steady electrical current (bias) acting onto the both magnets and i_c is the control current. On the other hand, the air gap in each magnet is given by:

$$g_1 = g_0 - x \quad ; \quad g_2 = g_0 + x \quad (4)$$

where g_0 is the nominal air gap assuming that the rotor is centered in the stator and x represents the displacement of the rotor from its centered position. Introducing Equations (3) and (4) in Equation (2), the control force can be calculated as follows:

$$F_N = \left(\frac{\varepsilon \mu_0 N^2 A_g i_s}{g_0^2} \right) i_c - \left(\frac{\varepsilon \mu_0 N^2 A_g i_s^2}{g_0^3} \right) x \quad (5)$$

Equation (5) was obtained assuming that the control current i_c and the displacement x is very small compared to the steady current i_s and the nominal air gap g_0, respectively, so that were neglected the higher-order terms of the control current and the displacement. As we can see, the magnetic forces change as a function of control current and gap thickness. The Equation (5) can conveniently be written as follows:

$$F_N = K_i i_c + K_x x \quad (6)$$

being K_i called the current stiffness and K_x is called the position stiffness.

B. ***Electrical current of control***

The control current is determined based on the displacement of the rotor. The equation that relates the position of the rotor with the control current (employing Laplace transforms) is given by:

$$i_c(s) = G(s)x(s) \quad (7)$$

being *G(s)* the overall transfer function of the control circuit, which is composed by multiplying the transfer functions of all components of the electronic control circuit, as follows:

$$G(s) = SE(s)LPF(s)PID(s)AMP(s) \quad (8)$$

where *SE*(*s*), *LPF*(*s*), *PID*(*s*) and *AMP*(*s*) are the transfer functions of the position sensor, low pass filter, PID controller and power amplifier, respectively. The classical models of transfer functions for these components of the control circuit are, [1]:

$$SE(s) = V_x(s) / x(s) \quad (9)$$

$$LPF(s) = \frac{\omega_{LP}^2}{s^2 + 2\xi_{LP}\omega_{LP}s + \omega_{LP}^2} \quad (10)$$

$$PID(s) = \frac{K_T\left(K_D s^2 + K_P s + K_I\right)}{s} \quad (11)$$

$$AM(s) = K_A \frac{\omega_A^2}{s^2 + \sqrt{2}\omega_A s + \omega_A^2} \quad (12)$$

being ω_{LP} and ξ_{LP} the cutoff frequency and damping ratio of the low pass filter; K_T, K_D, K_P and K_I are the total, derivative, proportional and integral gains of the PID controller; K_A and ω_A are the gain and cutoff frequency of the power amplifier.

Equation (8) can be further simplified by replacing the complex frequency $i\omega$ for the Laplace variable s to give:

$$G(\omega) = a_G(\omega) + ib_G(\omega) \quad (13)$$

in which $a_G(\omega)$ is the real part and $ib_G(\omega)$ is the imaginary part of the overall transfer function of the electronic circuit of control.

C. *Equivalent stiffness and damping*

Figure 3 shows the forces generated by the magnets, F_1 and F_2, acting onto the rotor in a single control axis. For this simplified model, the equation that describes the motion of the rotor at that point is given by:

$$M_r\ddot{x} + F_2 - F_1 = F_i \quad (14)$$

where M_r is the modal mass of the rotor at point where the bearing is placed. By introducing the Equations (6), (7) and (13) into Equation (14) and assuming harmonic forcing function acting onto the rotor, we can have the solution:

$$-M_r X\omega^2 + \left[K_x + K_i\left(a_G + ib_G\right)\right]X = \overline{F_i} \quad (15)$$

The equivalent stiffness and equivalent damping of the active magnetic bearings can be determined by equating the forces produced by these parameters (as shown in Equation (15)) with the forces of an equivalent system, i.e.:

$$\left(K_{eq} + C_{eq}i\omega\right)X = \left[K_x + K_i\left(a_G + ib_G\right)\right]X \quad (16)$$

From Equation (16), by equating the real and imaginary terms we obtain the equivalent stiffness and damping of the bearing, respectively, given by:

$$K_{eq} = K_x + K_i a_G \quad (17)$$

$$C_{eq} = \frac{K_i b_G}{\omega} \quad (18)$$

The equivalent stiffness and damping of the active magnetic bearings vary with frequency due to its dependence of the real and imaginary parts of the overall transfer function, which are also frequency dependents.

III. ROTOR-MAGNETIC BEARING MODEL

A simplified model for describing the vibration motions of the rotor-magnetic bearing was employed. The rotor is supported by two active magnetic bearing. A rigid disk is attached in the mid-span of the rotor allowing introducing unbalance force onto the system. The equation of motion of the vibration system can be described by:

$$[M]\{\ddot{x}(t)\} + [C]\{\dot{x}(t)\} + [K]\{x(t)\} = f(t) = \{F\}e^{i\omega t} \quad (19)$$

where [M], [C] and [K] are square N x N matrices ('N' being degree of freedom of system) and are usually referred to as the mass or inertia matrix, the damping matrix and the stiffness matrix, respectively; $f(t)$ is the harmonic exciting force due to unbalance mass and x is the generalized coordinate. The mass matrix [M] is obtained from the geometric characteristics of the rotor, [C] and [K] are obtained from Equations (17) and (18), and $f(t)$ is generated by an eccentric mass attached onto the rigid disk. Once the system is harmonically excited, the solution of Equation (19) is given by:

$$\{X\} = [Z(\omega)]^{-1}\{F\} \quad (20)$$

and the matrix $[Z(\omega)]$ is called the impedance matrix which can be determined from the terms of the mass, damping and stiffness matrices, as follows:

$$Z_{ij}(\omega) = -\omega^2 m_{ij} + i\omega c_{ij} + k_{ij} \;\; ; \; i,j = 1, 2, \ldots N \quad (21)$$

The time response to a given exciting frequency of the system is therefore obtained by equation:

$$\{x(t)\} = \{X\}e^{i\omega t} \quad (22)$$

The transmitted force to the bearing house, allowing X_p as the maximum amplitude of the rotor displacement at the nodal point where the magnetic bearing is placed is given by:

$$FT_p = X_p\sqrt{K_{eq}^2 + \left(\omega C_{eq}\right)^2}\, e^{i\omega t} \quad (23)$$

which should be equal to the control force required to keep the rotor in the centered position in the bearing, Equation (5).

IV. EXPERIMENTAL SET-UP

Figure 4 shows a picture of the experimental rotor apparatus in which the experimental analysis was carried out. The rotor is supported by two active magnetic bearings, which has a 620 mm long steel shaft with 19 mm in diameter and is driven by an electric motor through a flexible coupling. The rotor is capable of operating at rotating speed as high as 10,000 rpm. A steel rigid disk with holes for the placement of unbalance weights has been attached to the shaft at approximately mid-span location. The span between the bearings has 419 mm and the rigid disk has 1.75 kg in mass. An unbalance mass of 4.98 grams at eccentric distance of 50 mm was attached to the disk to generate unbalance exciting force on the system, as we can see in the Fig. 4. The PID controller is tuned by means of a user interface called MBScope provided by the manufacturer.

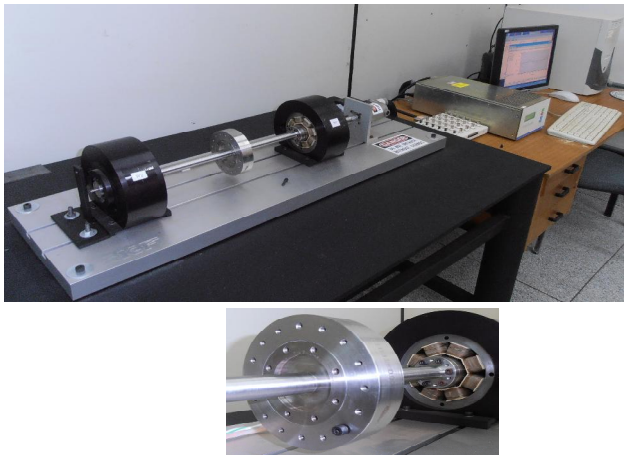

Fig. 4 Experimental rotor-magnetic bearings apparatus

Table 1 shows the design characteristics of the magnetic bearings and values of the PID controller parameters. The cutoff frequency and damping factor values of the low pass filter was taken 800 Hz and 0.7, respectively. The cutoff frequency of the power amplifier was taken the value of 20 kHz.

TABLE 1 DESIGN CHARACTERISITCS OF THE MAGNETIC BEARINGS

Parameters	Values	Parameters	Values
ε	*0.826*	*SE*	*5715 V/m*
μ_0	$4.\pi.10^{-7}$ Hm^{-1}	K_T	*0.00015*
A_q	$430.74x10^{-6}$ m^2	K_D	*0.015*
N	*276 coils*	K_P	*24*
i_s	*1.0 A*	K_I	*50*
g_0	$432x10^{-6}$ *m*	K_A	*142*

V. THEORETICAL RESULTS

The numerical simulations were accomplished using codes implemented in MatLab. According to Fig. 4, the active magnetic bearing (AMB) to the right (close to the drive motor) is called here AMB1 while the left bearing will be referred as AMB2. The analyzes were restricted to the frequency range from 0 to 2000 rpm, once to obtain the experimental data, higher rotating speeds with the unbalanced rotor are not recommended.

A. *Responses of the magnetic bearings*

Figure 5 shows the theoretical unbalance frequency responses of the rotor-magnetic bearings system in the analysis range. The results were obtained using the Equation (20) at the nodal points where the bearings are placed. Previous analyzes show that there is a critical speed in this range around 1370 rpm, which does not stand out due to the high modal damping, [12]. As we can see the frequency response at the AMB1 presents values higher than 40 μm and at the AMB2 reaches values higher than 60 μm.

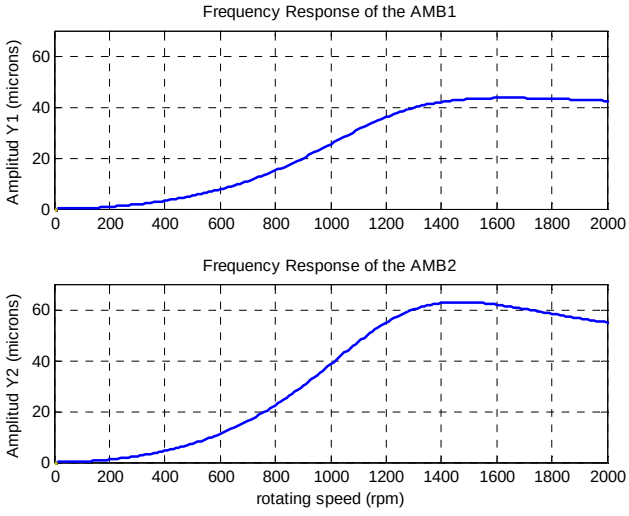

Fig. 5 Frequency response of rotor at AMB positions

The time unbalance responses of rotor at rotating speed of 2000 rpm are shown in Fig. 6, which were obtained through the Equation (22) at nodal points where the bearings are placed. The figure shows that the maximum amplitude at the AMB1 is 44.21 μm and the maximum amplitude at the AMB2 is 56.17 μm. The difference between the amplitudes of both bearings is because the rotor is not completely symmetrical.

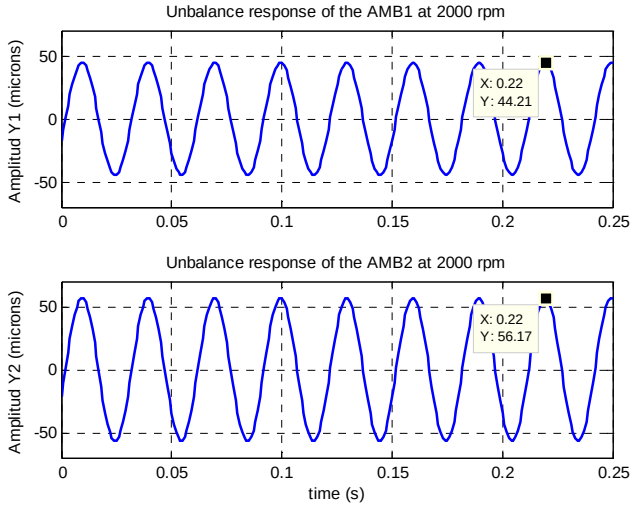

Fig. 6 Time unbalance response of rotor at AMBs positions – 2000 rpm

B. *Control currents of the magnetic bearings*

The frequency spectrum of the control current can be plotted by using the Equation (7) in frequency domain. It can be seen in Fig. 7 that the control current in the AMB1 exceeded 0.25 Amper while we have amplitudes higher than 0.35 Amper in the AMB2. The control current amplitudes generated at 2000 rpm are shown in Fig. 8, in which we can see the current of approximately 0.25 Amper in the AMB1 and the current of 0.323 Amper in the AMB2.

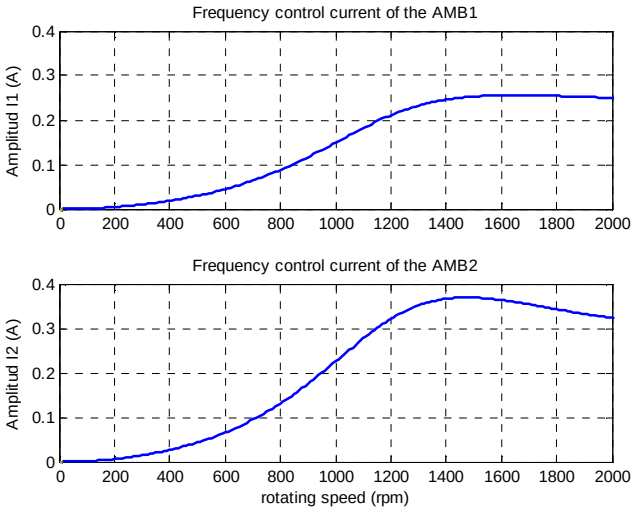

Fig. 7 Spectrum of control current generated in the magnetic bearings

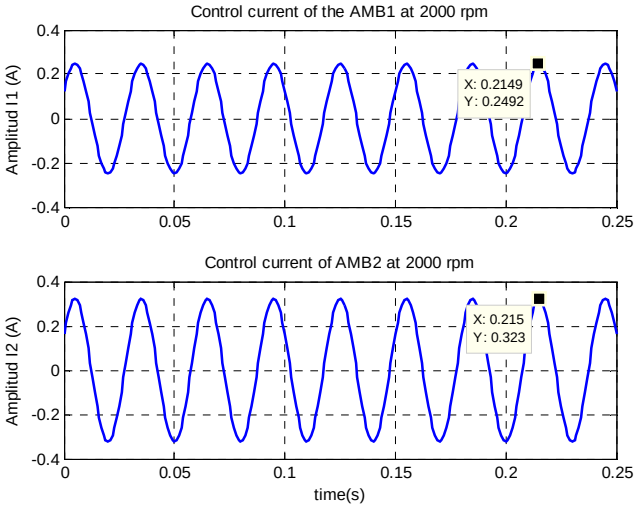

Fig. 8 Control current generated in the magnetic bearings at 2000 rpm

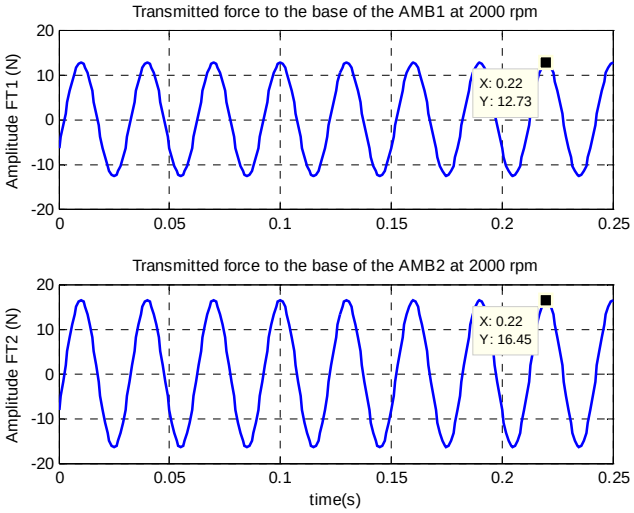

Fig. 10. Transmitted forces in the magnetic bearing houses at 2000 rpm

C. *Control and transmitted forces of the magnetic bearings*

The control forces were calculated using the Equation (5) from the magnetism physics principles. As we can see in Fig. 9, the maximum control forces to keep the rotor at the centered position of the bearings were 13.83 N and 17.87 N for the AMB1 and AMB2, respectively. Note that these are values of forces needed to control the rotor spinning at 2000 rpm. On the other hand, the Fig. 10 indicates the transmitted forces to the bearing houses obtained by using the Equation (23) from the mathematical model. It is found that the value of the maximum transmitted force from the AMB1 is of 12.73 N and from the AMB2 is of 16.45 N. The control forces are slightly higher than the transmitted forces, but the difference is not more than 8%, ensuring good accuracy in the force simulations.

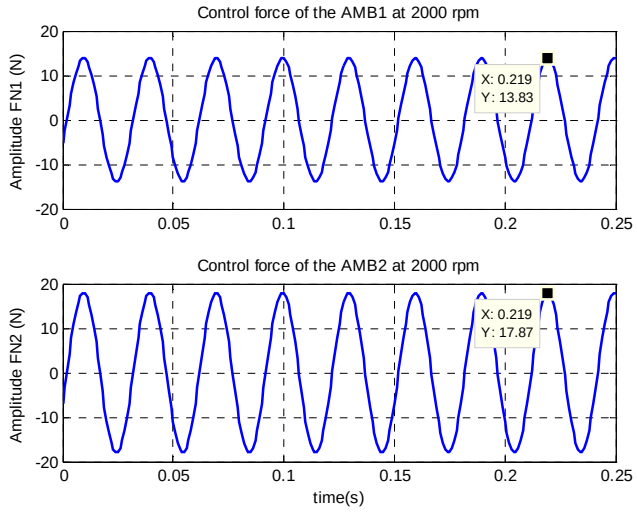

Fig. 9 Control forces in the magnetic bearings at 2000 rpm

VI. EXPERIMENTAL RESULTS

The experimental results were obtained from the rotor system shown in Fig. 4. The rotor operates assisted by a microcomputer through the software which provides a friendly user interface, allowing controlling the rotor rotating speed, presenting graphics of displacements and currents, orbits and others. The experimental data were captured during rotor start up until it reaches 2000 rpm. As already mentioned, to operate the unbalanced rotor at running speeds above 2000 rpm is not recommended and high displacements triggers a protection device causing rotor coast-down.

A. *Experimental responses of the magnetic bearings*

To analyze the experimental data the residual unbalance of the rotor and the residual current to control was initially found. Fig. 11 shows the residual rotor unbalance during start up. As can be seen, the residual unbalance is very small, producing no more than 8 μm of displacement on both magnetic bearing. As a consequence, the residual control current also resulted very small, no more than 0.03 Amper in start up. The time to the rotor reaches 2000 rpm is about 10 seconds, at an acceleration of 200 rev/sec.

Figure 12 presents the experimental frequency unbalance responses at AMBs positions in start up condition. One can verify that there is a good correlation of these results with the theoretical results seen in Fig. 5, even being included in the amplitude the cumulative error due to rotor residual unbalance. At running speed of 2000 rpm the amplitudes of rotor are 42.9 μm and 54.65 μm at AMB1 and AMB2, respectively, as indicated by the curves in Fig 13. Comparing these results with those shown in Fig. 6, it can be seen a great approximation between the experimental results and simulation results, with errors around 3%.

This approach between the experimental and simulated results indicates satisfactory accuracy of the procedure to calculate the equivalent stiffness and damping of the active magnetic bearings, according to Equations (17) and (18), including the estimation of the overall transfer function of the control circuit given by Equation (13). Also, the simplified

model was enough in representing dynamically the rotor system.

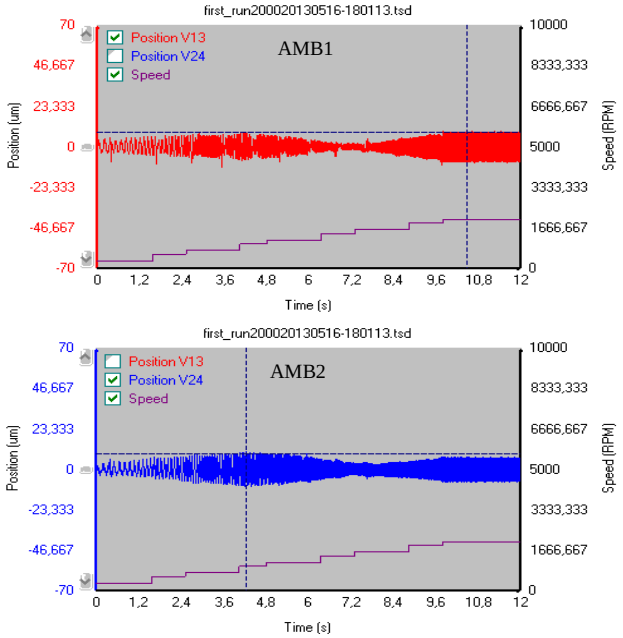

Fig. 11 Residual unbalance of rotor in the start up

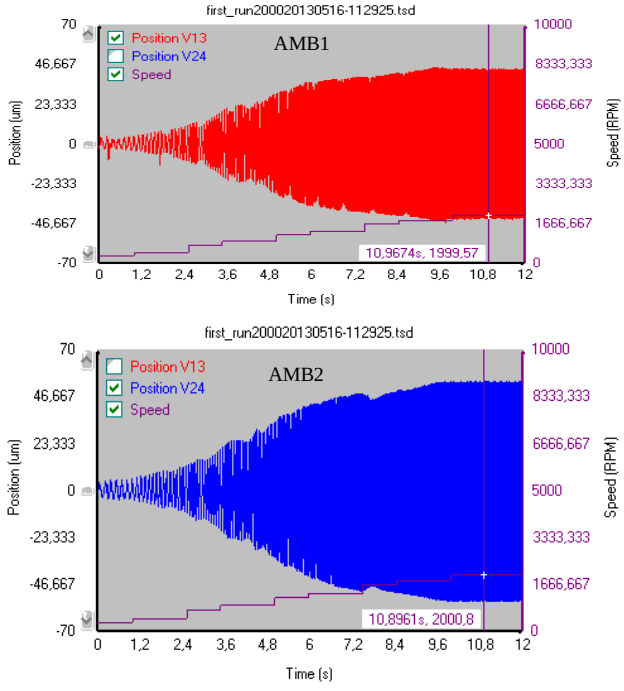

Fig. 12 Experimental frequency response of rotor at AMBs positions

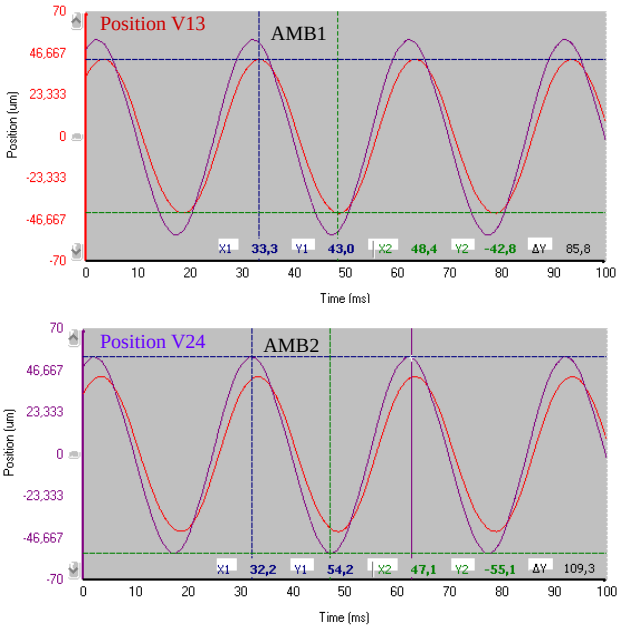

Fig. 13 Experimental time unbalance response of rotor at AMBs positions – 2000 rpm

B. ***Experimental control currents of the magnetic bearings***

Figure 14 shows the experimental control current frequency spectrum in start up of rotor. The steady offset levels observed in the curves represent the steady electrical current (bias) acting onto the bearings (in this case 1.0 Amper) plus the constant current level due to the effect of the own weight of the rotor, since these results were obtained from the top magnets (top current). At the bottom magnets, the steady offsets levels (not shown here) correspond to the steady electrical current (bias) less the electrical current due to the own weight of the rotor.

The experimental results shown in Fig. 14 indicate smaller control current amplitudes in the AMB1 respect to the amplitudes in the AMB2 in the range analyzed. These results also present a significant correlation with the simulation results in Fig. 7. At running speed of 2000 rpm, the control current to keep the rotor in centered position of the bearings are 0.2 Amper and 0.25 Amper to the AMB1 and AMB2, respectively, as indicated by the curves plotted in Fig. 15. By comparing these results with those shown in Fig. 8, it can be seen that the simulated results of both bearings are higher than the experimental results, presenting errors of 24.6% and 29.2% for the AMB1 and AMB2, respectively.

In part, these errors can be attributed to the effect of the residual control current previously mentioned, as well as due to the cumulative error of the simulated control current, once it depends on the displacement, Equation (7), which also introduces certain error. Therefore, it is considered that the procedure to calculate the control current of active magnetic bearings proposed in this work can be safely used, with acceptable errors.

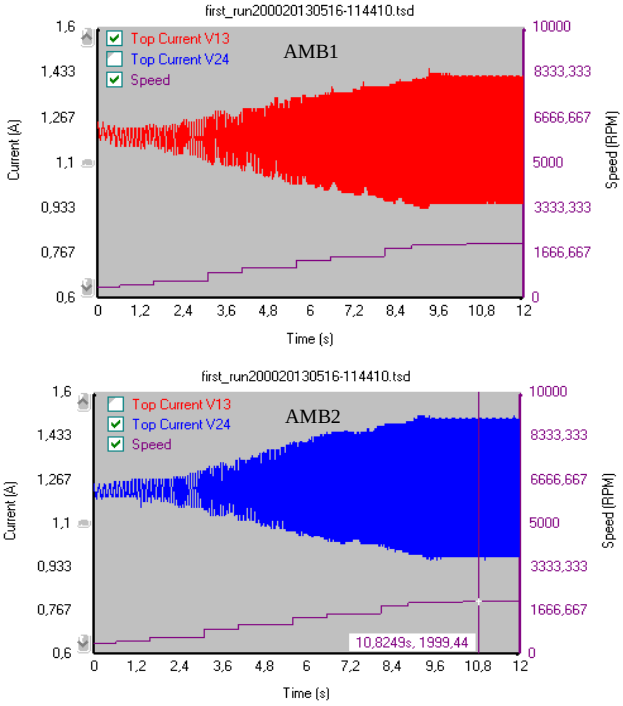

Fig. 14 Experimental spectrum of control current generated in the magnetic bearings

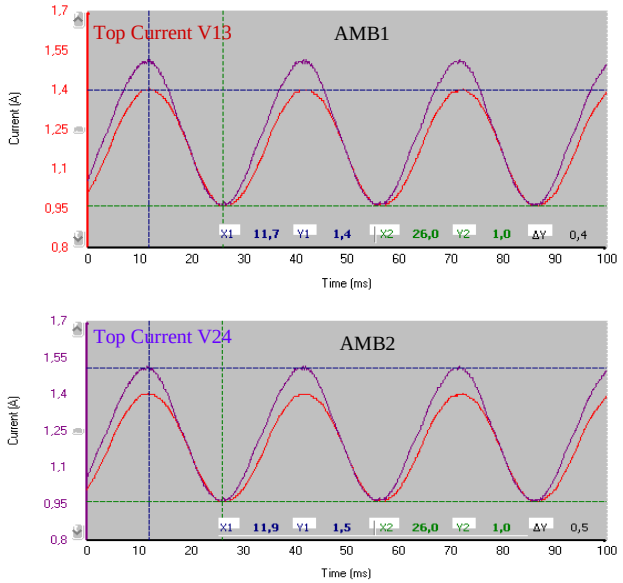

Fig. 15 Experimental control current generated in the magnetic bearings at 2000 rpm

VII. FINAL REMARKS

A procedure to calculate the electrical control current and control force of active magnetic bearings is presented. The control current depends basically on the overall transfer function of the control circuit and the displacement of the rotor within the bearing housing. The control force depends basically on the design features of the magnetic bearing as well as the control current and displacement of the rotor. Simulated unbalance frequency response and control current frequency response were obtained by a simplified model developed for an experimental rotor-magnetic bearings. Time unbalance response and time control current at rotating speed of 2000 rpm also were simulated. These results were compared with experimental data acquired from the rotor-magnetic bearings excited by unbalance force.

In terms of displacement, there was an important approach between simulated and experimental results, indicating that the model has satisfactory accuracy in dynamically representing the rotor. This precision is needed since both control force and control current depends on the displacement.

Concerning the control electrical current, the procedure for its determination through the overall transfer function and the displacement of the rotor produced values sufficiently accurate. The errors respect to the experimental data were as expected.

The procedure for calculating the control force showed consistent, providing value close to the force transmitted to the base of the magnetic bearings, ensuring the accuracy of the method. Unfortunately the rotor test does not provide the control force values directly to undertake a theoretical and experimental comparison.

ACKNOWLEDGMENT

The authors would like to thank São Paulo State Research Council (FAPESP-Brazil) and INCT-CNPq-FAPEMIG to support this work research.

REFERENCES

[1] Allaire, P.E., Maslen, E.H., Humphris, R.R., Lewis, D.W., "Magnetic Bearings. STLE Handbook of Tribology and Lubrication", Vol. III, Charlottesville, USA, 1993.

[2] Kasarda, M.E.F., "An overview of active magnetic bearing technology and application". In The Shock and Vibration Digest, Vol. 32, N.2, pp. 91-99, 2000.

[3] Schweitzer, G. and Maslen, E.H., " Magnetic bearings: theory, design, and application to rotating machinery", Springer-Verlag Berlin Heidelberg, 2009.

[4] Kuseyri, I.S., "Robust control and unbalance compensation of rotor/active magnetic bearing", Journal of Vibration and Control, Vol. 18(6), pp 817-832, 2011.

[5] Shi, J., Zmood, R. and Qin, L., "Synchronous disturbance attenuation in magnetic bearing systems using adaptive compensating signals", Control Engineering Practice, Vol. 12, pp. 283-290, 2004.

[6] Piper, G.E., Watkins, J.M. and Thorp III, O.G., "Active control of axial-flow fan noise using magnetic bearings", Journal of Vibration and Control, Vol. 11(9), pp. 1221-1232, 2005.

[7] Jang, M., Chen, C. and Tsao, Y., "Sliding mode control for active magnetic bearing system with flexible rotor", Journal of the Franklin Institute, Vol. 342, pp. 401-419, 2005.

[8] Zhu, C., Robb, D.A. and Ewins, D.J., "The dynamics of a cracked rotor with an active magnetic bearing", Journal of Sound and Vibration, Vol. 265, pp. 469-487, 2003.

[9] Cole, M.O.T., Keogh, P.S., Sahinkaya, M.N. and Burrows, C.R., "Towards fault-tolerant active control of rotor-magnetic bearing systems", Control Engineering Practice, Vol. 12, pp. 491-501, 2004.

[10] Schweitzer, G., "Active magnetic bearings – chances and limitations", International Centre for Magnetic Bearings, ETH Zurich,

[11] Zingerli, C.M., Kolar, J.W., "Novel observer based force control for active magnetic bearings", The 2010 International Power Electronics Conference, ETH Zurich, 2010.

[12] Nascimento, L.P., "Análisis dinámica teórica y experimental de un rotor con cojinetes magnéticos activos", VII Congreso Bolivariano de Ingeniería Mecánica, Cusco, Peru, 2012.